Bull. Mater. Sci. (2022)45:113
https://doi.org/10.1007/s12034-022-02690-9

Electro-optical properties improvement of organic composite using p-nitro-benzylidenemalonotrile-based small organic molecules

ASMA MILED[1,*], HAMZA SAIDI[1], HASSEN DHIFAOUI[1], RIADH HANNACHI[2] and ABDELAZIZ BOUAZIZI[1]

[1]Equipe Dispositifs Electroniques Organiques et Photovoltaïque Moléculaire, Laboratoire de la Matière Condensée et des Nanosciences, Faculté des Sciences de Monastir, Université de Monastir, Avenue de l'Environnement, 5019 Monastir, Tunisia

[2]Laboratoire des Energies et des Matériaux (LabEM), Institut Supérieur d'Informatique et des Techniques de Communication, Université de Sousse, 4011 Hammam Sousse, Tunisia

*Author for correspondence (asma.miled08@gmail.com)

MS received 17 June 2021; accepted 11 February 2022

Abstract. The solution-processable small organic molecules have turned into one of the most promising semiconductors due to their exclusive properties in the inexpensive optoelectronic field. In this work, we report the study of the incorporation effect of the small organic molecules of p-nitro-benzylidenemalonotrile (NO_2-BMN) into conjugated polymer poly(3-hexylthiophene) (P3HT) on the optical and electrical properties. The UV–visible and photoluminescence (PL) responses were performed to confirm the enhancement of the optical properties. PL results showed that P3HT: NO_2-BMN composite with (1:1.25) ratio has the best charge transfer efficiency that occurs between both compounds. The current–voltage characteristics through dark J (V) revealed that the ITO/P3HT: NO_2 BMN/Al structure had a diode behaviour with a relatively low threshold voltage (V_{th}). We have estimated the different electrical parameters such as the saturation current, barrier high (Φ_b) and the ideality factor (n). Moreover, we have evaluated the different charge transport mechanisms by the analyses of J–V characteristics in a double logarithmic scale under dark conditions. The obtained results proved that the incorporation of NO_2-BMN enhances the electrical properties of the composite.

Keywords. π-Conjugated small organic molecules; p-nitrobenzylidenemalonotrile; P3HT; charge transfer; electrical characteristics.

1. Introduction

Π-conjugated small organic molecules have received great interest to the researchers in the field of organic optoelectronic devices, not just because of its tunable opto-electrochemical properties, but also because of its flexibility, solution processability and low cost [1–6]. Moreover, this category of n-type organic molecules had a good ability to accept electrons owing to the conjugated structure, which is a basic property for materials in photovoltaic applications. Recently, tremendous efforts have been devoted to the synthesis and the development of semiconductor materials based on benzylidenemalononitrile (BMN) units [7,8]. It has generated respectable attention as electron-deficient building units of synthetic organic chemical applications. Substitution on the BMN unit plays a crucial role to tune the optical and electronic characteristics of conjugated small molecules [9]. Moreover, introducing strong electron-withdrawing groups such as the nitro group on the BMN unit results in decreasing the highest-occupied molecular orbital (HOMO) and the lowest-unoccupied molecular orbital (LUMO) energy levels, and enhancing the electron-accepting ability of the corresponding molecule [10,11]. As is known, the nitro group has high electronegativity. In our previous work, we synthesized a conjugated small molecule of p-nitro-benzylidenemalononitrile (NO_2-BMN) and its electrochemical and optical characteristics were investigated. The obtained results make them a promising candidate for utilizing as the electron acceptor material of the composite devices [12]. It is interesting to explore and study the NO_2-BMN molecules in composite reinforcement materials. Therefore, in this study, we have incorporated the NO_2-BMN into the polymeric matrix of P3HT to form a donor–acceptor composite system. P3HT is one of the most widely used donor polymers in optoelectronic devices and organic solar cells due to its good solubility in various solvents, high absorption coefficient, environmental stability and high charge mobility [13–16]. The effect of NO_2-BMN concentration on the optoelectrical characteristics of the composite device was investigated.

Published online: 25 June 2022

2. Experimental

2.1 *Material*

Indium tin oxide (ITO) glass substrates with a sheet resistance of 20 Ω cm^{-1} and poly(3-hexyltiophene) (P3HT) with a molecular weight of 77.500 g mol^{-1} were purchased from Ossila. p-Nitrobenzylidenemalonotrile (NO_2-BMN) was synthesized in our laboratory. For the synthesis of NO_2-BMN, we prepare 50 ml of a mixture of the solution containing one equivalent of malononitrile and one equivalent of 4-nitrobenzaldehyde in toluene. After that, we add 0.1 ml of glacial acetic acid and 0.05 ml of a catalytic amount of piperidine. The mixed solution was refluxed overnight with a water trap (Dean-Stark) until no further water was separated. The solvent was removed under reduced pressure and the residue was taken up in Et_2O. Then, was washed with HCl (50 ml, 5%) and washed several times with water followed by drying ($MgSO_4$). The residue was further purified by recrystallization from a pentane/ethyl acetate mixture [17]. The kinetics of alkaline hydrolysis of p-substituted benzylidenemalononitriles was studied in previous work [9]. All the materials were used as received without any further purification. Figure 1a presents the chemical structure of P3HT and NO_2-BMN.

2.2 *Device fabrication and characterization techniques*

For the preparation of the different devices based on ITO/P3HT: NO_2-BMN/Al, we have first cleaned ITO substrates by ultra-sonication for 15 min in acetone, isopropyl alcohol (IPA) and deionized water, then dried with nitrogen gas. P3HT and NO_2-BMN were dissolved in chloroform and were made in different weight ratios: (1:0, 1:0.25, 1:0.5, 1:1 and 1:1.25). The mixed solutions were stirred for 4 h at room temperature. After that, solutions were deposited onto ITO glass substrates by spin coating at 3000 rpm for 20 s, which gives the same film thickness for all devices. Finally, an aluminium cathode was deposited by thermal evaporation under a vacuum of 10^{-6}. Figure 1b and c show the device structure and the energy level diagram of the ITO/P3HT: NO_2-BMN/Al device.

UV–visible absorption was recorded using a Perkin Elmer lambda 35 UV-Vis spectrophotometer. The photoluminescence (PL) spectra were measured at room temperature using Jobin Yvon-spex spectrum CCD detector. The excitation source used is a laser with a wavelength equal to 375 nm. *J–V* characteristics of the different elaborated devices were measured using a computer-controlled Keithley 6430 source Measure Unit.

3. Results and discussions

In the aim to investigate the changes in the optical properties upon the incorporation of the N O_2-BMN into the polymer matrix P3HT, the UV–vis absorption spectra of pristine P3HT and P3HT: NO_2-BMN composite in thin films with different NO_2-BMN concentrations (1:0, 1:0.25, 1:0.5, 1:1 and 1:1.25) were measured and are presented in figure 2. The absorption spectrum of P3HT film shows a board absorption band in the wavelength range of 350–650 nm with the presence of three peaks at 524, 553 and 605 nm. The first peak provides information on the degree of conjugation in the P3HT chains, while the second shoulders are related to the interchain order [18]. Upon incorporation of NO_2-BMN, we noted broadening of absorption spectra in the UV–vis regions, with the same spectral profile that of the pristine polymer. This is originated from the absorption of NO_2-BMN pristine. As can be seen in the inset of figure 2, the NO_2-BMN film shows two strong absorption bands between 339–428 nm and 524–830 nm. The first band is related to the π-π* transition of the benzene ring. While

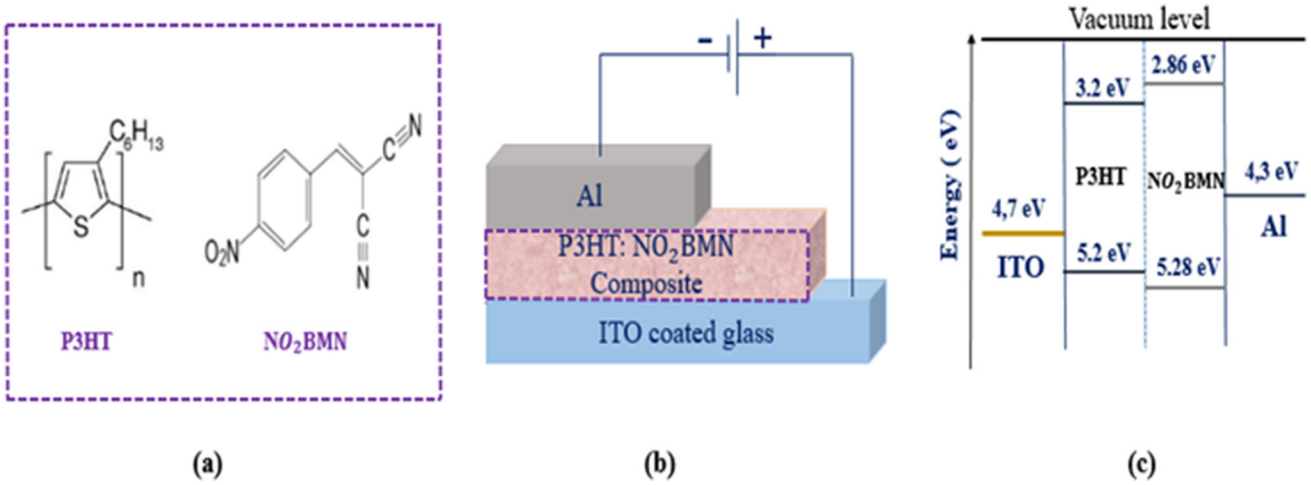

Figure 1. (**a**) Chemical structure of P3HT and NO_2-BMN, (**b**) typical schematic diagram of the device structure and (**c**) the energy level diagram of the ITO/P3HT: NO_2-BMN/Al device.

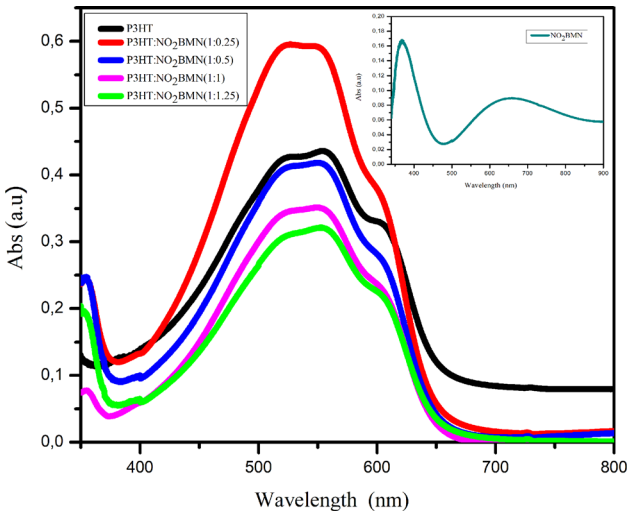

Figure 2. Absorption spectra of pristine P3HT and P3HT: NO_2-BMN composite thin films for different concentrations of NO_2-BMN. The inset shows the absorption spectrum of NO_2-BMN film.

the second one is related to the n-π* transition of the nitro group (NO_2) conjugated with the aromatic rings. Interestingly, the composite with (1:0.25) ratio exhibits a significant increase in the absorption intensity, which can be explained by an increase in the optical volume of the P3HT. In contrast, a gradual decrease in the absorption intensity with an increase of the NO_2-BMN content in the polymer is observed. This result could be attributed to the reduction in the optical volume of P3HT in composite films [19].

The charge transfer properties of different composite films containing various amounts of NO_2-BMN were studied by performing the PL measurements under the excitation of 375 nm (figure 3). The PL spectrum for the pristine P3HT shows two strong PL emission peaks at 662 and 708 nm attributed to intra-chain and inter-chain radiative recombination of the exciton in P3HT molecules [20]. It is

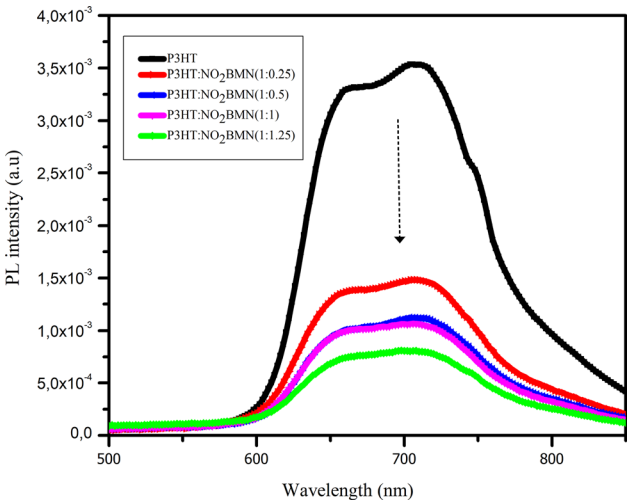

Figure 3. PL spectra of pristine P3HT and P3HT: NO_2-BMN composite films.

remarkable that the addition of NO_2-BMN into the P3HT matrix gradually decreases the PL intensity. This is due to charge transfer that occurred between polythiophene chains and p-nitro-benzylidenemalonotrile molecules [21]. Moreover, this result proves the existence of a more dissociation interface leading to the enhancement of the exciton dissociation, and this will affect electrical characteristics.

To extract the optimal weight ratio of P3HT: NO_2-BMN, we have evaluated the amount of charge transfer by using the following equation [22]:

$$\eta = 1 - \frac{I}{I_0}, \tag{1}$$

where I_0 and I are the PL intensities before and after the introduction of the acceptor molecules, respectively. From the calculated η values (table 1), it is clear that η increases with the increasing proportion of NO_2-BMN in the polymer matrix and attains the maximum value of 76% for P3HT: NO_2-BMN (1:1.25). We can therefore deduce that P3HT: NO_2-BMN (1:1.25) presents the optimal composition for an effective charge transfer between the donor and acceptor materials.

To well understand the concentration effect on charge transportation properties, the electrical properties were studied via *J* (*V*) characteristics in the dark of ITO/P3HT/Al and ITO/ P3HT: NO_2-BMN/Al. Figure 4 shows a rectifying behaviour that is typically observed in the Schottky diode. The shape of the different devices exhibits a slow variation of the reverse current with the applied voltage, while the forward current increases exponentially with the voltage. Moreover, we found that the incorporation of NO_2-BMN in the polymer matrix leads to the reduction of the threshold voltage V_{th} and the improvement of the current density. This result may be attributed to the enhancement in the charge transport due to the formation of a conducting pathway by the incorporation of NO_2-BMN into P3HT [23].

Various diode parameters have been extracted by using the *J*–*V* curves with the Schottky theory, in which the current can be expressed as [24]:

$$J = J_s\left[\exp\left(\frac{qV}{nK_BT}\right) - 1\right], \tag{2}$$

here, q denotes the electronic charge, V is the applied voltage, K_B is Boltzmann constant, T is the absolute

Table 1. Charge transfer parameter *vs.* different amounts of NO_2-BMN within P3HT polymer matrix.

Samples	I/I_0	η
P3HT	1	0
P3HT: NO_2 BMN (1:0.25)	0.4	0.60
P3HT: NO_2 BMN (1:0.5)	0.32	0.68
P3HT: NO_2 BMN (1:1)	0.29	0.71
P3HT: NO_2 BMN (1:1.25)	0.24	0.76

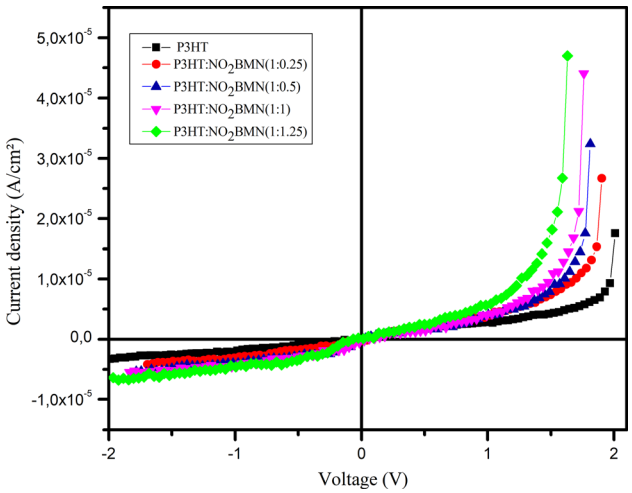

Figure 4. Dark *J–V* characteristics in the linear scale of devices based on ITO/P3HT: NO_2-BMN/Al for different concentrations of NO_2-BMN.

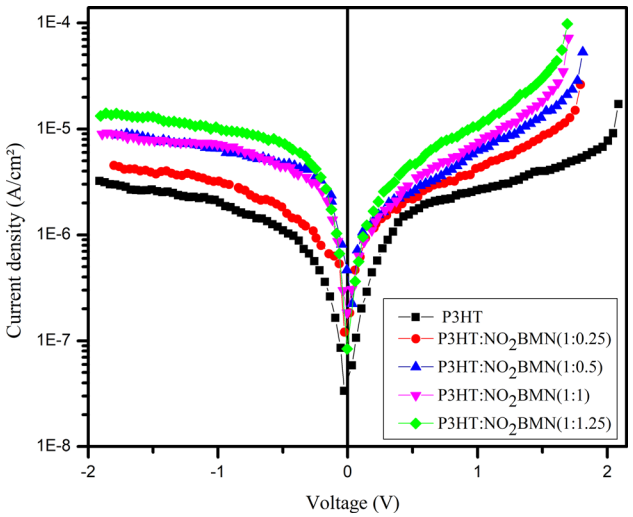

Figure 5. Dark *J–V* characteristics in the semi-logarithmic scale of devices based ITO/P3HT: NO_2-BMN/Al for different concentrations of NO_2-BMN.

temperature, n the ideality factor and J_s is the current saturation that can be calculated by using the following relation:

$$J_s = A^* T^2 \exp\left(\frac{-q\Phi_b}{K_B T}\right), \tag{3}$$

where A^* is the Richardson constant (120 A cm^{-2} K^{-2} taken from Richardson's law) and Φ_b is the barrier high at zero bias.

Using the above equations, the ideality factor and barrier high can be expressed as:

$$n = \frac{q}{K_B T}\left(\frac{dV}{d\ln J}\right), \tag{4}$$

$$\Phi_b = \frac{K_B T}{q}\left(\frac{\ln(A^* T^2)}{J_s}\right). \tag{5}$$

In addition, n and J_s can be determined from the slopes and the current axis intercepts of linear regions of the *J–V* characteristics presented in semi-logarithmic plots (figure 5), respectively.

The obtained values are summarized in table 2. We note from table 2 that all the device's electrical parameters are dependent on the NO_2-BMN concentration. We found that the effective barrier height decreases with the increasing the NO_2-BMN content. This result may be due to the decrease of LUMO and HOMO levels of polymer P3HT with the incorporation of NO_2-BMN. This variation in LUMO level of P3HT around the ITO Fermi level causes the decrease of function difference between ITO and the active layer [25]. Furthermore, the decrease of Φ_b contributes to the improvement of charge transfer at the P3HT/NO_2-BMN interface. Indeed, electrons can easily surmount the barrier resulting in the quenching of the PL intensity as shown above. On the other hand, we found that the value of the ideality factor n of all the devices is higher than 1. This might be related to various phenomena such as the presence of the interface defects due to the poor contact formation leading to the generation-recombination process, barrier inhomogeneity at the polymer/Al interface, carrier leakage and the series resistance [26]. P3HT: NO_2 BMN (1:1.25) based device presents the lowest value of ideality factor (n) among the different devices under study, which is equal to 2.27. This result may be attributed to the reduction of the generation-recombination rate of electrons and holes leading to the improvement in charge mobility and injection, which enhances the current density. These findings are consistent with the PL measurement results.

The high values of the ideality factor indicate the existence of another charge transport mechanism different to thermionic emission. In this context, to identify the dominant current conduction mechanism, we have analysed the double logarithmic plots of *J–V* characteristics of all the elaborated devices with different concentrations of NO_2-BMN in dark conditions. As can be observed in figure 6, it is clear that all the devices show typical power-law dependence $I = V^m$. Here, m provides information about the dominant charge transport mechanism and the m values are determined from the slope of measured data by linear fit [27]. According to this behaviour, all the *J–V* curves can be divided into two distinct regions as presented in figure 6. At low voltage, a linear dependence of J (V) ($m \sim 1$) is observed. This suggests that the conduction is governed by the Ohmic, in which the density of thermally generated charge carriers in the active layer dominate injected charge carriers from electrodes. The current density in this region is given by ohm's law, which is defined by the following formula [28]:

$$J = qn_0\mu\frac{V}{d}, \tag{6}$$

Table 2. Diode parameters obtained from *I–V* curves of the devices with different concentrations of NO_2-BMN.

ITO/P3HT: NO_2 BMN/Al	1:0	1:0.25	1:0.5	1:1	1:1.25
V_{th} (V)	1.93	1.74	1.64	1.60	1.48
I_s (A)	1.033×10^{-6}	1.32×10^{-6}	1.35×10^{-6}	1.50×10^{-6}	2.27×10^{-6}
Φ_b	0.773	0.767	0.766	0.763	0.753
n	4.34	3.13	2.65	2.34	2.27

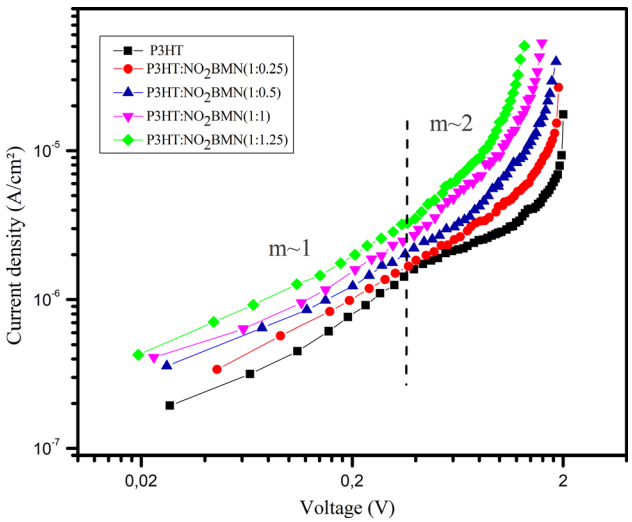

Figure 6. *J–V* characteristics of ITO/P3HT: NO_2-BMN/Al structure in double logarithmic scale for different weight ratios of NO_2-BMN under dark conditions.

where $n_0, \mu, q$and d are the free carrier density, charge mobility, electronic charge and thickness of the active layer.

At higher bias voltage, we observe a quadratic variation of the current as a function of the applied voltage ($m \sim 2$). This region corresponds to the space charge limited conduction behaviour, which is due to the superiority of the charge injected from the contact than the thermally generated carriers. The current density is expressed as follows [29]:

$$J = \frac{9}{8}\varepsilon_r \theta \mu \frac{V^2}{d^3}, \tag{7}$$

where ε_r is the permittivity of the organic semi-conductor and θ the trap factor which is written as $\theta = \frac{p_0}{p_0 + p_t}$, where p_0 and p_t are the densities of free carrier and the trapped hole, respectively.

4. Conclusions

To summarize, P3HT: NO_2-BMN composite films with various weight ratios (1:0, 1:0.25, 1:0.5, 1:1 and 1:1.25) were successfully elaborated using the spin coating method. Optical characterization showed that the addition of NO_2-BMN affects the charge transfer. PL results proved that P3HT: NO_2-BMN (1:1.25) present the optimal weight ratio for an effective charge transfer. Similarly, J (V) measurements in the dark showed that the incorporation of NO_2-BMN improves the electrical properties of P3HT: NO_2-BMN composite. Indeed, there was a decrease in the threshold voltage V_{th}, the height of the load injection barrier Φ_b and the ideality factor n with an improvement in the current density.

References

[1] Chen J, Chen Y, Feng W, Gu C, Li G, Su N *et al* 2020 *Energy Chem.* **2** 100042
[2] Dhifaoui H, Aloui W, Saidi H, Bouazizi A and Boubaker T 2019 *Mater. Res. Express.* **6** 086310
[3] Xue P, Dai S, Lau T, Yu J, Zhou J, Xiao Y *et al* 2020 *Sol. RRL* **4** 2000115
[4] Luo M, Zhu C, Yuan J, Zhou L, Keshtov M L, Godovsky D Y *et al* 2019 *Chin. Chem. Lett.* **30** 2343
[5] Kan B, Kan Y, Zuo L, Shi X and Gao K 2021 *Info. Mat.* **3** 175
[6] Yadav A, Upadhyaya A, Gupta S K and Negi C M S 2020 *Phys. E: Low-Dimens. Syst. Nanostruct.* **124** 114351
[7] Aloui W, Dhahri N, Bouazizi A, Boubaker T and Goumont R 2016 *Superlattices Microstruct.* **91** 302
[8] Dhifaoui H, Aloui W and Bouazizi A 2020 *Mater. Res. Express.* **7** 045101
[9] Dhahri N, Taoufik B and Goumont R 2014 *J. Phys. Org. Chem.* **27** 484
[10] Morais Eduardo M, Grillo Igor B, Stassen Hubert K, Seferin M and Jackson D 2018 *New J. Chem.* **42** 10774
[11] Saidi H, Dhahri N, Aloui W, Bouazizi A, Boubaker T and Goumont R 2018 *Superlattices Microstruct.* **120** 193
[12] Saidi H, Aloui W, Dhifaoui H, Bouazizi A and Boubaker T 2019 *J. Mater. Sci.: Mater. Electron.* **30** 10808
[13] Saini V, Abdulrazzaq O, Bourdo S, Dervishi E, Petre A, Bairi V G *et al* 2012 *J. Appl. Phys.* **112** 054327
[14] Hajlaoui M E, Hnainia N, Gouid Z, Benchaabane A, Sanhoury M A and Chtourou R 2020 *Mater. Sci. Semicond. Process.* **109** 104934
[15] Yang C, Yu R, Liu C, Li H, Zhang S and Hou J 2021 *Chem. Sus. Chem.*. https://doi.org/10.1002/cssc.202100627
[16] Mousavi S L, Jamali Sheini F, Sabaeian M and Yousefi R 2020 *Sol. Energy* **199** 872

[17] Corson B B and Stoughton R W 1928 *J. Am. Chem. Soc.* **50** 2825
[18] Kadem B Y, Kadhim R G and Banimuslem H 2018 *J. Mater. Sci. Mater.* **29** 9418
[19] Arranz Andrés J and Blau W J 2008 *Carbon* **46** 2067
[20] Chang S H, Chiang C H, Cheng H M, Tai C Y and Wu C G 2013 *Opt. Lett.* **38** 5342
[21] Mhamdi A, Ltaief A and Bouazizi A 2017 *J. Mol. Struct.* **1145** 81
[22] Chehata N, Ltaief A, Ilahi B, Salem B, Bouazizi A, Maaref H *et al* 2014 *J. Lumin.* **156** 30
[23] Sharma N, Negi C M S, Verma A S and Gupta S K 2018 *J. Electron. Mater.* **47** 7023
[24] Dhifaoui H, Aloui W, Hannachi R, Bouazizi A and Boubaker T 2021 *Optik* **226** 166028
[25] Yadav A, Upadhyaya A, Gupta S K, Verma A S and Negi C M S 2019 *Thin Solid Films* **675** 128
[26] Yadav A, Upadhyaya A, Gupta S K and Negi C M S 2020 *Phys. E: Low-Dimens. Syst. Nanostructures.* **124** 114351
[27] Rathore P, Negi C M S, Yadav A, Verma A S and Gupta S K 2018 *Optik* **160** 131
[28] Rathore P, Negi C M S, Verma A S, Singh A, Chauhan G, Inigo A R *et al* 2017 *Mater. Res. Express.* **4** 085905
[29] Sweii F B S, Bkakri R, Aloui W and Bouazizi A 2019 *J. Mater. Sci.: Mater. Electron.* **30** 20823